Pergamon

Control Eng. Practice, Vol. 5, No. 6, pp. 791-800, 1997

0967-0661/97 $17.00 + 0.00

PII0967-0661(97)00063-4

IMPLEMENTATION OF DAMPED-RATE RESOLVED-ACCELERATION ROBOT CONTROL

Sun-Li Wu and Shir-Kuan Lin

Institute of Control Engineering, National Chiao Tung University, Hsinchu 300, Taiwan, ROC

(Received September 1996; in final form March 1997)

Abstract: The damped least-squares method has frequently been used to solve the singularity problem of resolved-acceleration control schemes. It works by damping only the joint accelerations, so that the joint accelerations in the degenerated directions (the end-effector cannot move along these directions) are zero at a singular point. However, the joint velocities in the degenerated directions may be nonzero in some situations, in which case they will create fluctuations around the singular point. In this paper, a damped-rate resolved-acceleration control scheme (DRRAC) is proposed to overcome this drawback. The paper also shows that the DRRAC is asymptotically stable, and its convergent property is discussed. Experiments were undertaken to verify the proposed control scheme.

Keywords: Robot control, resolved-acceleration control, singularities, damped least-squares method.

1. INTRODUCTION

Resolved-rate control and resolved-acceleration control (Luh, *et al.*, 1980) are two general control schemes for the control of robots in Cartesian space. The resolved-rate control scheme is suitable only for low-speed motion control, since it ignores the manipulator dynamics. This paper, however, considers only the resolved-acceleration control scheme, which is known to break down when the Jacobian matrix is singular. In the neighborhood of the singularity, very large joint speeds are required to produce small changes in some end-effector positions or orientations.

An effective strategy that allows motion control of the manipulator in the neighborhood of singularities is the damped least-squares method, originally proposed by Nakamura and Hanafusa (1986) and Wampler (1986).

Most researchers in this area (Chiaverini, 1993; Chiaverini, *et al.*, 1994; Maciejewski and Klein, 1988) have used the damped least-squares method to solve the singular problem of the resolved-rate control scheme. An overview of the damped least-squares method for inverse kinematics of manipulators was presented by Deo and Walker (1995). Wampler and Leifer (1988) presented the application of the damped least-squares method to both the resolved-rate control scheme and the resolved-acceleration control scheme.

In this paper the resolved-acceleration control scheme using the damped least-squares method is named "damped-acceleration resolved-acceleration control scheme" (DARAC). Lin and Wu (1995) proposed a degenerated-direction

version of the damped least-squares method to deal with the singularity of the resolved-acceleration control scheme. They first tried to find the degenerated directions of a manipulator, and then applied the damped least-squares method only in these directions, while the accuracy of the motion along the other directions was maintained. Lin and Wu also pointed out in their experiments that there were fluctuations around the workspace boundary for the DARAC if the target was at the unreachable region (i.e., outside the workspace).

In industry, robot operators seldom know what the singular point is, or where it is. The workspace boundary of nonredundant manipulators is composed of the singular points. The operators may therefore ask the end-effector to pass outside the workspace, and then fluctuations will occur around the boundary of the workspace. These fluctuations may make the system unstable.

Another problem of the DARAC is self-motion (Lin and Wu, 1995). The motions of the joints which produce no movement of the end-effector are referred to as self-motion. When the self-motion occurs, some joints will rotate indefinitely, thus exceeding their limits.

In this paper, the singular value decomposition (SVD) is used to show that the fluctuations and the self-motion are due to the unnecessary nonzero joint velocities in the degenerated directions when the manipulator is at a singularity. The *damped-rate* resolved-acceleration control (DRRAC) is proposed to remove these unnecessary joint velocities. The example of a two-link arm will illustrate the physical characteristics of this control law. The fluctuations and the self-motion in DARAC are remedied, at the cost of an insignificantly small error in a long decaying period, if the target is in the neighborhood of a singularity. The stability is studied by means of Lyapunov's second method. Finally, the proposed control scheme is implemented on a PUMA 560 manipulator, and is tested by three experiments.

This paper is organized as follows. The resolved-acceleration control scheme and the damped least-squares method are reviewed in Section 2. Section 3 analyzes the performance of the DARAC in a neighborhood of a singular point, the results of which motivate the formulation of the DRRAC scheme. A two-link arm illustrates the physical insights gained. The stability analysis is presented in Section 4. Some experiments concerning motion near the singularities are reported in Section 5, and conclusions are drawn in the final section.

2. BACKGROUND

2.1 *Resolved-acceleration control*

The relationship between the end-effector velocities and the joint rates for robotic manipulators can be represented as

$$\dot{x} \equiv \begin{bmatrix} \dot{r} \\ \boldsymbol{\omega} \end{bmatrix} = J\dot{q} \tag{1}$$

where $\dot{r}$ and $\boldsymbol{\omega}$ are the end-effector velocity and the angular velocity, respectively, $\dot{q}$ is the joint rate vector, and J is the Jacobian matrix. Differentiating eq. (1) gives

$$a \equiv \begin{bmatrix} \ddot{r} \\ \boldsymbol{\alpha} \end{bmatrix} = J\ddot{q} + \dot{J}\dot{q} \tag{2}$$

where $\ddot{r}$ and $\boldsymbol{\alpha}$ are the end-effector acceleration and the angular acceleration, respectively.

It is well-known that the dynamics of a manipulator can be modelled in the form of

$$M(q)\ddot{q} + f(\dot{q}, q) = \boldsymbol{\tau} \tag{3}$$

where $M(q)$ is the positive definite, symmetric inertia matrix, $f(\dot{q}, q)$ is the vector comprising Coriolis, centrifugal and gravity forces, $\boldsymbol{\tau}$ is the vector of the actuator forces, and q is the vector of joint displacements. The second-order nonlinear coupled dynamic equation (3) can be linearized and decoupled by inputting the inverse dynamics:

$$\boldsymbol{\tau} = M(q)\ddot{q}^* + f(\dot{q}, q) \tag{4}$$

where $\ddot{q}^*$ is the vector of the desired joint accelerations, so that

$$\ddot{q} = \ddot{q}^*. \tag{5}$$

That means that by adding the inverse dynamics as a compensator in a conventional controller, the trajectory tracking in the joint coordinates is then guaranteed. This technique is called the *computed torque* scheme.

Luh, *et al.* (1980) proposed the resolved-acceleration control scheme as

$$\ddot{q}^* = J^{-1}a^* = J^{-1}\left(\begin{bmatrix} \ddot{r}_d \\ \boldsymbol{\alpha}_d \end{bmatrix} + K_D \begin{bmatrix} \dot{r}_d - \dot{r} \\ \boldsymbol{\omega}_d - \boldsymbol{\omega} \end{bmatrix} + K_P \begin{bmatrix} \boldsymbol{\epsilon}_r \\ \boldsymbol{\epsilon}_e \end{bmatrix} - \dot{J}\dot{q}\right). \tag{6}$$

K_D and K_P are gain matrices, subscript "d" denotes the desired value, $\boldsymbol{\epsilon}_r = r_d - r$ is the positional error, and $\boldsymbol{\epsilon}_e$ is the orientation error. The orientation error can be θu, $u\tan\theta/2$ (Rodrigues parameters), $u\sin\theta$ (the parameters of Luh, *et*

al.), or $u \sin\theta/2$ (Euler parameters), where θ is the rotational angle, and u is the unit vector of the rotational axis (Lin, 1995). Unfortunately, this control scheme breaks down when J^{-1} does not exist, which occurs at a singular configuration.

2.2 *Damped least-squares method*

The damped least-squares method for the inverse problem of eq. (1) is applied to solve the following optimization problem (Nakamura and Hanafusa, 1986; Wampler, 1986):

$$\min_{\dot{q}}(\| J\dot{q} - \dot{x} \|^2 + \rho^2 \| \dot{q} \|^2) \tag{7}$$

where ρ is the damping factor. The solution to eq. (7) is

$$\dot{q}_\rho = J_\rho^\dagger \dot{x} \tag{8}$$

where

$$J_\rho^\dagger = (J^T J + \rho^2 I)^{-1} J^T \tag{9}$$

which always exists for $\rho \neq 0$. This solution is a compromise between the residual error, $J\dot{q} - \dot{x}$, and the magnitudes of the joint velocities, $\dot{q}$, by ρ.

The singular value decomposition (SVD) can provide an insight into the singularities of the inverse Jacobian (Maciejewski and Klein, 1989). This paper deals with nonredundant manipulators, so J is a 6×6 matrix. By the theory of SVD, there are two orthogonal matrices $U = [u_1 \cdots u_6]$ and $V = [v_1 \cdots v_6]$, such that

$$J = U\Sigma V^T = \sum_{i=1}^{6} \sigma_i u_i v_i^T \tag{10}$$

where $\Sigma = \mathrm{diag}[\sigma_1, \ldots, \sigma_6]$, σ_i are the singular values of J. The vectors u_i and v_i are the i-th left singular vector and the i-th right singular vector, respectively. Substituting eq. (10) into (9) gives

$$J_\rho^\dagger = V\Sigma_\rho^\dagger U^T = \sum_{i=1}^{6} \frac{\sigma_i}{\sigma_i^2 + \rho^2} v_i u_i^T \tag{11}$$

where $\Sigma_\rho^\dagger = \mathrm{diag}[\sigma_1/(\sigma_1^2 + \rho^2), \ldots, \sigma_6/(\sigma_6^2 + \rho^2)]$.

Suppose that ρ is moderately small. When the manipulator is far from a singularity (i.e., $\sigma_i \gg \rho$), then $\sigma_i/(\sigma_i^2 + \rho^2) \approx 1/\sigma_i$, which implies that $J_\rho^\dagger \approx J^{-1}$ (see eq. (11)). When the manipulator is in a neighborhood of a singular point, it can be seen from eq. (11) that the solutions of the joint velocities $\dot{q}$ are not infinitely large.

J^{-1} in eq. (6) is replaced by $J_\rho^\dagger$ to obtain the following control scheme (Kirćanski, *et al.*, 1994; Lin and Wu, 1995):

$$\ddot{q}_{da}^* = J_\rho^\dagger a^* = \sum_{i=1}^{6} \frac{\sigma_i}{\sigma_i^2 + \rho^2} (u_i^T a^*) v_i. \tag{12}$$

The vector $\ddot{q}_{da}^*$ in eq. (12) is actually the solution to the optimization problem of

$$\min_{\ddot{q}^*}(\| J\ddot{q}^* - a^* \|^2 + \rho^2 \| \ddot{q}^* \|^2). \tag{13}$$

The control scheme given by eq. (12) is referred to as DARAC. Note that if an ideal computed-torque control is used, the joint acceleration $\ddot{q}$ is equal to $\ddot{q}_{da}^*$, by eq. (5).

Wampler and Leifer (1988) proposed another optimization problem as

$$\min_{\ddot{q}}(\| J\ddot{q}^* - a^* \|^2 + \rho^2 \| \ddot{q} + C\dot{q} \|^2) \tag{14}$$

where $C = K_d I + B$, $B(q,t)$ is a positive-definite symmetric damping matrix. In their literature, the stability was proved; however, the solution of this optimization problem was not solved, and the choice of the damping factor ρ and the damping matrix B was omitted.

3. DAMPED-RATE CONTROL SCHEME

3.1 *Motivation*

In this section, the motion problem of the DARAC in the neighborhood of a singularity is stated, and the reason for this problem is analyzed. First, from eq. (12), it is known that any vectors in the joint space can be represented as a linear combination of the right singular vectors $v_1, \ldots, v_6$. And the vectors in Cartesian space can be represented as a linear combination of the left singular vectors $u_1, \ldots, u_6$. Thus, in eq. (6), a^* can be represented as

$$a^* = \sum_{i=1}^{6} \lambda_i u_i. \tag{15}$$

Substituting eqs (11) and (15) into (12) gives

$$\ddot{q}_{da}^* = \sum_{i=1}^{6} \gamma_i v_i \tag{16}$$

where $\gamma_i = \sigma_i \lambda_i / (\sigma_i^2 + \rho^2)$.

Applying the DARAC, if the manipulator is at the singularity, say $\sigma_k = 0$, then $\gamma_k = 0$, since

$\gamma_k = \sigma_k\lambda_k/(\sigma_k^2 + \rho^2)$. This implies that the component of $\ddot{q}_{da}^*$ along v_k is zero. Thus, the component of $\ddot{q}$ along v_k is zero by eq. (5) if an ideal computed torque control is used. In this configuration, the component of $\dot{q}$ along v_k is uncontrollable, i.e., the value of $\dot{q}$ along v_k cannot be changed. This component of $\dot{q}$ may be nonzero in some situations. In general, if the target is outside the workspace, or there is an unreachable region between the initial position and the desired position, the component of $\dot{q}$ along v_k is nonzero when the end-effector approaches the workspace boundary containing the singular point $\sigma_k = 0$. These nonzero components of $\dot{q}$ are unnecessary, and will create some problems, which can be stated as follows.

The degeneration (or singularity) of a manipulator with a spherical wrist can be classified into two parts: wrist-center degeneration and orientation degeneration. In the following discussion, the problems of the DARAC in these two degeneration configurations will be shown.

(1) The wrist-center degeneration: Consider a two-link arm, shown in Fig. 1(a), whose symbolic singular value decomposition of the Jacobian matrix can be found in (Kirćanski and Borić, 1993). From there, the second left singular vector is

$$u_2 = \begin{bmatrix} -\text{sign}(S_2 p)C_{12}u_{21} - S_{12}u_{22} \\ -\text{sign}(S_2 p)S_{12}u_{21} + C_{12}u_{22} \end{bmatrix} \quad (17)$$

where

$$\begin{aligned} S_2 &= \sin\theta_2, \\ S_{12} &= \sin(\theta_1 + \theta_2), \\ C_{12} &= \cos(\theta_1 + \theta_2), \\ p &= l_1 + l_2, \\ u_{21} &= \sigma_1\sqrt{l_2^2 - \sigma_2^2}/(l_2\sqrt{\sigma_1^2 - \sigma_2^2}), \\ u_{22} &= \sigma_2\sqrt{\sigma_1^2 - l_2^2}/(l_2\sqrt{\sigma_1^2 - \sigma_2^2}). \end{aligned}$$

Equations (15) and (16) are rewritten as

$$a^* = \lambda_1 u_1 + \lambda_2 u_2 \quad (18)$$

$$\ddot{q}_{da}^* = \frac{\sigma_1\lambda_1}{\sigma_1^2 + \rho^2}v_1 + \frac{\sigma_2\lambda_2}{\sigma_2^2 + \rho^2}v_2. \quad (19)$$

The tip of the two-link arm will move from a point $\boldsymbol{A}$ on the y-axis to a target point that is also on y-axis and outside the workspace. When the tip reaches the singular point $\boldsymbol{B}$ on the boundary of the workspace (see Fig. 1(b)), then $u_2 = [0 \ -1]^T$ and λ_2 is nonzero, since the positional error along u_2 is nonzero. However, the component of $\ddot{q}_{da}^*$ along v_2 is forced to zero since $\sigma_2 = 0$ (see eq. (19)). Then the component of $\ddot{q}$ along v_2 will

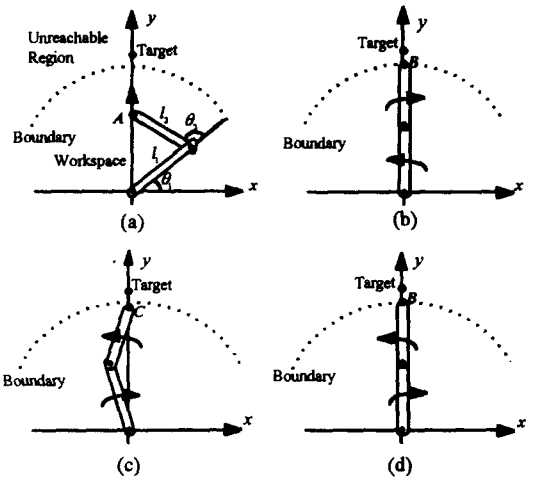

Fig. 1. The motion of a two-link arm from (a), (b), (c) to (d) through the singular point $\boldsymbol{B}$.

become zero by eq. (5) if an ideal computed-torque control is used. The component of $\dot{q}$ along v_2 is nonzero, since this component of $\dot{q}$ was not properly decelerated. So, link 1 moves continuously in a counterclockwise direction, and link 2 moves in a clockwise direction. Thus, the tip is drawn from the singular point $\boldsymbol{B}$ to point $\boldsymbol{C}$ (Fig. 1(c)). As this happens, the controller will command the arm to return to the target; link 1 then moves in a clockwise direction and link 2 in a counterclockwise direction. When the tip returns to the singular point $\boldsymbol{B}$ (Fig. 1(d)), the velocities of the two links will remain nonzero, and the tip will then leave the singular point $\boldsymbol{B}$ again. Clearly, slowly decaying fluctuations do occur around the singular point $\boldsymbol{B}$.

(2) The orientation degeneration: Consider the spherical wrist that is shown in Fig. 2. The singularity occurs when the first and third rotational axes are colinear, i.e., the angle of the second joint is zero. In this configuration, the component of the angular velocity of the wrist, along the first rotational axis, can be achieved by infinite combinations of the joint velocities of the first and

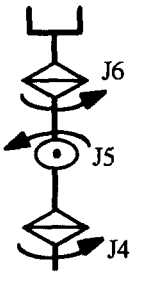

Fig. 2. The spherical wrist.

third axes, since one of these two joint velocities can be cancelled by the other in the opposite direction. Suppose the spherical wrist is ordered to stay in the singular configuration. When the angle of the second joint approaches zero, the joint accelerations of the first and third joints also approach zero, controlled by the DARAC. At the same time, the joint velocities of the first and third joints are uncontrollable. If one of these two joint velocities is nonzero, due to an external torque or a numerical error in the controller computation, the other joint will rotate at the same speed in the opposite direction. As the controller cannot stop them since they are uncontrollable, these two joints will rotate indefinitely in the singular configuration.

3.2 *The damped-rate resolved-acceleration control scheme*

The above analysis reveals that a good robot Cartesian control scheme should restrict the joint velocities as well as the joint accelerations. If the joint velocities are restricted, then so are the joint accelerations. The converse is, however, not true. This concept motivated the formulation of a control scheme that solves the following optimization problem:

$$\min_{\ddot{q}^*}(\| J\ddot{q}^* - a^* \|^2 + \rho_r^2 \| \dot{q}^* \|^2). \tag{20}$$

In order to solve the solutions of this optimization problem in a closed form, the discrete-time technique was used. In discrete-time control, the back difference is always used to approximate the derivative, so that

$$\ddot{q}^*(k) = \frac{1}{\Delta t}(\dot{q}^*(k) - \dot{q}^*(k-1)) \tag{21}$$

where Δt is the sampling time. Note that, by the assumption of ideal computed-torque control, the measured value of $\dot{q}(k)$ in this sampling interval is equal to the command $\dot{q}^*(k-1)$ in the last sampling interval. Then

$$\ddot{q}^*(k) = \frac{1}{\Delta t}(\dot{q}^*(k) - \dot{q}(k)). \tag{22}$$

For convenience, the index k is dropped in the subsequent expressions; hence eq. (22) becomes

$$\ddot{q}^* = \frac{1}{\Delta t}(\dot{q}^* - \dot{q}). \tag{23}$$

Substituting eq. (23) into (20), the solution of the optimization problem (20) is

$$\ddot{q}^*_{dr} = J^\dagger_{\rho_r}(a^* + \frac{1}{\Delta t}J\dot{q}) - \frac{1}{\Delta t}\dot{q} \tag{24}$$

where the damping factor $\rho_r \equiv \rho\Delta t$. Equation (24) is the control law of the DRRAC.

Actually, the DRRAC (24) has one more term than the DARAC (12). Equation (24) is rewritten as

$$\begin{aligned}\ddot{q}^*_{dr} &= \ddot{q}^*_{da} + \ddot{q}^*_c \\ &= J^\dagger_{\rho_r}a^* - \frac{\rho_r^2}{\Delta t}(J^TJ + \rho_r^2 I)^{-1}\dot{q}.\end{aligned} \tag{25}$$

If ρ_r is equal to ρ of the DARAC, then the first term on the right-hand side in the above equation is equal to the solution of the DARAC, and the second term on the right-hand side ($\ddot{q}^*_c$) is an additional term from the DRRAC. $\ddot{q}^*_c$ is rewritten in terms of the singular value decomposition of J as

$$\ddot{q}^*_c = \frac{1}{\Delta t}\sum_{i=1}^{6}\frac{-\rho_r^2}{\sigma_i^2 + \rho_r^2}(v_i^T\dot{q})v_i. \tag{26}$$

If the manipulator is far away from any singular point, i.e., $\sigma_i \gg \rho_r > 0$, $\rho_r^2/(\sigma_i^2 + \rho_r^2) \approx 0$, $i = 1, \ldots, 6$, $\ddot{q}^*_c$ is zero, and then the DRRAC is identical to the DARAC. When the manipulator is near or at the singular point, $\sigma_i \gg \rho_r > 0, i = 1, \ldots, k$ and $\sigma_j \cong 0, j = k+1, \ldots, 6$. Then eq. (26) can be reduced to

$$\ddot{q}^*_c \approx \frac{-1}{\Delta t}\sum_{i=k+1}^{6}(v_i^T\dot{q})v_i. \tag{27}$$

$\ddot{q}^*_c$ is the sum of the negative multiples of the components of $\dot{q}$ along $v_{k+1}, \ldots, v_6$. From the discussion in the last section, it can be deduced that the components of $\dot{q}$ along $v_j, j = k+1, \ldots, 6$, are unnecessary. The DRRAC uses $\ddot{q}^*_c$ to remove the unnecessary components of $\dot{q}$.

3.3 *Illustration for a two-link arm*

A two-link arm was simulated under control by the DARAC and the DRRAC, to observe the performance of the two control schemes. The lengths of the first and second links were 0.55 m and 0.45 m, respectively. The initial position of the tip was (0, 0.5). The controller parameters were defined as follows: $K_P = 100I$, $K_D = 20I$, the sampling period was 5 ms. ρ of the DARAC and ρ_r of the DRRAC were both chosen for these simulations as in the case (Lin and Wu, 1995)

$$0.02e^{-1250(\sigma_{min}-0.02)^2} \tag{28}$$

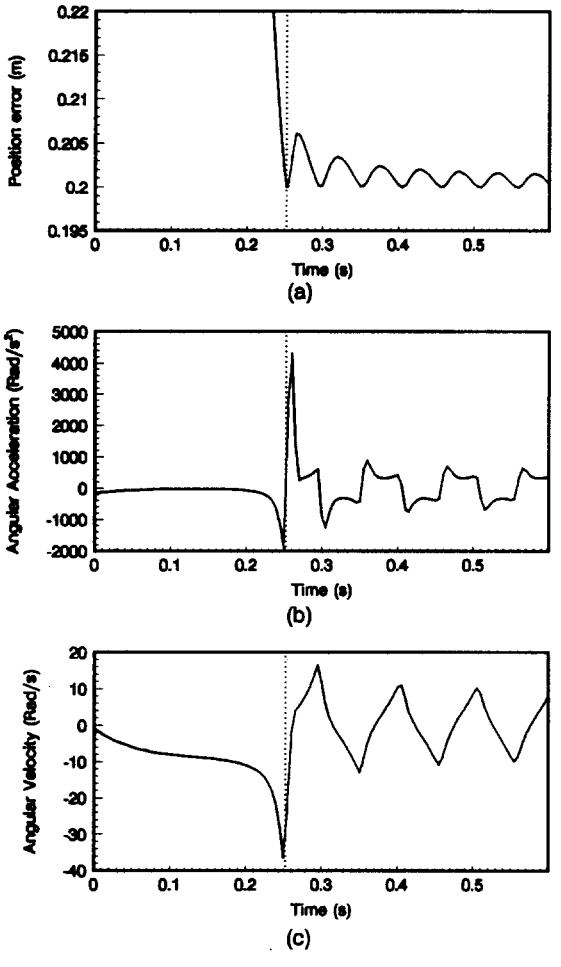

Fig. 3. The simulation results with DARAC, when the target is outside the workspace: (a) positional error, (b) $v_2^T\ddot{q}$, (c) $v_2^T\dot{q}$.

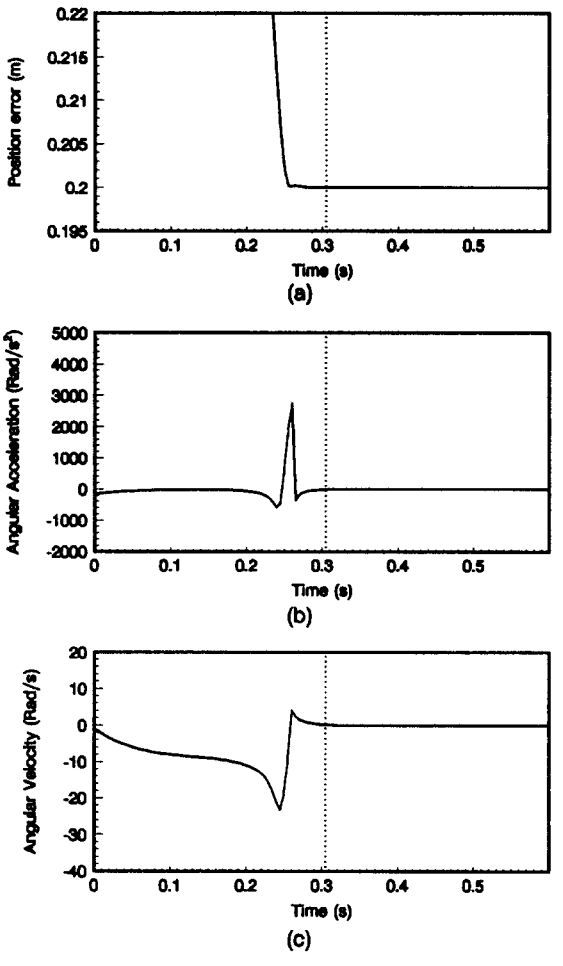

Fig. 4. The simulation results with DRRAC, when the target is outside the workspace: (a) positional error, (b) $v_2^T\ddot{q}$, (c) $v_2^T\dot{q}$.

where σ_{min} is the smallest singular value of J.

Initially, the two control schemes were simulated for the target position outside the workspace. The target position was set (0, 1.2). Note that (0, 1) is a singular point. The simulation results of the DARAC and the DRRAC are shown in Figs 3 and 4, respectively. Figs 3 (a), (b), and (c) are the positional errors, $v_2^T\ddot{q}$, and $v_2^T\dot{q}$, respectively, when using the DARAC. At $t = 0.252$ sec., the tip first reached a singular point (see Fig. 3 (a)) and $v_2^T\ddot{q}$ was damped to zero (see Fig. 3 (b)). However, at the same time, since $v_2^T\dot{q}$ was nonzero (see Fig. 3 (b)), the fluctuations occurred. On the other hand, when using the DRRAC, the tip reached the singular point at $t = 0.305$ sec. (see Fig. 4 (a)) and both $v_2^T\ddot{q}$ and $v_2^T\dot{q}$ (see Fig. 4 (c), (d)) were damped to zero at the same time, so no fluctuation occurred. These simulation results demonstrate that the DRRAC overcomes the fluctuation problem of the DARAC. Another simulation illustrated the phenomenon when the target position was at a singular point. The target position was set to (0, 1). The positional errors of the DARAC and the DRRAC are shown in Fig. 5. From this figure, it can be seen that the convergent rate of the DRRAC is slower than that of the DARAC when the tip is near the singular point. The DRRAC requires a very long time to reach the singular target, although the positional error is almost insignificantly small after 2 seconds. The same phenomenon occurs when the target is in the neighborhood of a singular point. The reason for this phenomenon is that the joint velocity along the degenerated direction, v_2, was damped when the tip was close to the singular point. This damped region is around the boundary of the workspace, and the size of this region depends on the damping factor. Fortunately, the size of the damped region is insignificantly smaller than that of the overall workspace, so that the DRRAC is still useful in terms of practical applications.

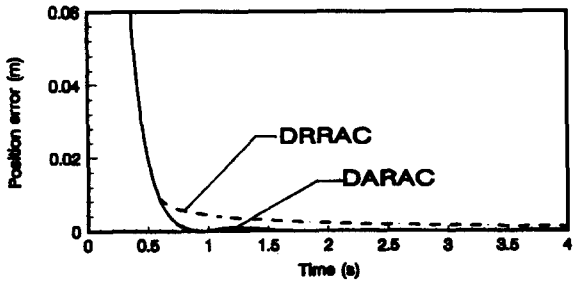

Fig. 5. The positional errors of DARAC and DRRAC for a target at a singular point.

4. STABILITY ANALYSIS

This section will show that the DRRAC is asymptotically stable, and will discuss its convergent property.

theoremTheorem Let the orientation error be $\epsilon_e = f(\theta_e)u_e$, where u_e and θ_e are, respectively, the rotational axis and the angle from the current orientation to the desired one, and

$$f(\theta_e) = \begin{cases} \theta_e, \\ \tan\dfrac{\theta_e}{2}, \\ \sin\theta_e, \\ \sin\dfrac{\theta_e}{2}. \end{cases}$$

Suppose that $\rho_r > 0$ when the manipulator is at the singular point. A sufficient condition for the global asymptotic convergence of the DRRAC in the whole workspace of the robot under the situation of $\ddot{r}_d = \dot{r}_d = 0$ and $\alpha_d = \omega_d = 0$ is that K_D is a positive-definite matrix and

$$K_P = \begin{bmatrix} k_{pr}I_3 & 0 \\ 0 & k_{pe}I_3 \end{bmatrix}.$$

k_{pr} and k_{pe} are positive. The equilibrium is at the point where $\dot{q} = 0$. *Proof:* Let a Lyapunov function be

$$L(q,\dot{q}) = \frac{1}{2}k_{pr}\epsilon_r^T\epsilon_r + k_{pe}E + \frac{1}{2}\dot{q}^T(J^TJ + \rho_r^2 I_6)\dot{q} \qquad (29)$$

where

$$\epsilon_r = r_d - r \qquad (30)$$

$$E = \int_0^{\theta_e} f(\phi)d\phi$$

$$\equiv \begin{cases} \dfrac{\theta_e^2}{2}, & \text{for} f(\phi) = \phi, \\ -2\ln|\cos\dfrac{\theta_e}{2}|, & \text{for} f(\phi) = \tan\dfrac{\phi}{2}, \\ 1-\cos\theta_e, & \text{for} f(\phi) = \sin\phi, \\ 2(1-\cos\dfrac{\theta_e}{2}), & \text{for} f(\phi) = \sin\dfrac{\phi}{2}. \end{cases} \qquad (31)$$

Clearly, $L(q,\dot{q}) \geq 0$. It is recognized that $\dot{\theta}_e = u_e \cdot (\omega_d - \omega)$ (see Table 1 in the literature of Spring, 1986). Differentiating E in eq. (31) obtains

$$\dot{E} = \frac{\partial E}{\partial \theta_e}\dot{\theta}_e = \epsilon_e \cdot (\omega_d - \omega). \qquad (32)$$

Evaluating $\partial L/\partial t$ along solutions of (29) yields:

$$\frac{\partial L}{\partial t} = k_{pr}\epsilon_r^T(\dot{r}_d - \dot{r}) + k_{pe}f(\theta_e)u_e^T(\omega_d - \omega) + \dot{q}^T(J^TJ + \rho_r^2 I_6)\ddot{q} + \dot{q}^T\dot{J}^TJ\dot{q}. \qquad (33)$$

If the ideal computed-torque control is used, $\ddot{q} = \ddot{q}^*$, then eq. (25) can be substituted into (33), giving

$$\frac{\partial L}{\partial t} = k_{pr}\epsilon_r^T\dot{r}_d + k_{pe}\epsilon_e^T\omega_d + \dot{q}^TJ^T\begin{bmatrix}\ddot{r}_d \\ \alpha_d\end{bmatrix} + \dot{q}^TJ^TK_D\left(\begin{bmatrix}\dot{r}_d \\ \omega_d\end{bmatrix} - J\dot{q}\right) - \frac{1}{\Delta t}\rho_r^2\dot{q}^T\dot{q}. \qquad (34)$$

If $\ddot{r}_d = \dot{r}_d = 0$ and $\alpha_d = \omega_d = 0$, then

$$\frac{\partial L}{\partial t} = -\dot{q}^TJ^TK_DJ\dot{q} - \frac{1}{\Delta t}\rho_r^2\dot{q}^T\dot{q}. \qquad (35)$$

Since K_D is a positive-definite matrix, $\partial L/\partial t \leq 0$ for all $\dot{q}$ and $\partial L/\partial t = 0$ only for $\dot{q} = 0$.

Combining the above results and $L(q,\dot{q}) \geq 0$, one can say, by the Lyapunov theorem, that $\dot{q}$ is asymptotically stable and the equilibrium point is $\dot{q} = 0$.

If the DARAC is used and the Lyapunov function also adopts eq. (29), then

$$\frac{\partial L}{\partial t} = -\dot{q}^TJ^TK_DJ\dot{q}. \qquad (36)$$

When the manipulator is at the singular point, $\sigma_{k+1} = \cdots = \sigma_6 = 0$, and $\dot{q}$ is spanned by v_i, $i = k+1,\ldots,6$, then $\partial L/\partial t = 0$. This implies that the equilibrium solution of the DARAC may be $\dot{q} \neq 0$ when the manipulator is at the singular point. However, $\partial L/\partial t$ for the DRRAC has an additional term $(-(1/\Delta t)\rho_r^2\dot{q}^T\dot{q})$ more than that of the DARAC to ensure that $\partial L/\partial t$ is zero only for $\dot{q} = 0$, i.e., the equilibrium solution of the

DRRAC is $\dot{q} = 0$.

The equilibrium solution $\dot{q} = 0$ suggests that all joints are stationary as $t \to \infty$ and

(1) if the target position is in the workspace or at the workspace boundary, the Lyapunov function L will decrease to zero as $t \to \infty$, i.e., the final position and orientation errors will be zero;
(2) if the target position is outside the workspace, L will decrease to a constant as $t \to \infty$. This means that the end-effector will converge to a singular point which is at the boundary and the target position is in the degenerated direction. The positional error cannot continue to decrease.

5. IMPLEMENTATION AND EXPERIMENTAL RESULTS

A modular integrated robot control system (MIRCS) (Wu and Lin, 1994) is used to implement the DARAC and the DRRAC on the PUMA 560 six-joint robot. Because the values of the inertia parameters are unavailable from the manufacturer, it has been impossible to implement the computed-torque scheme in the laboratory. Instead, a robust independent joint controller (Hsia, *et al.*, 1991; Tsai and Lin, 1990) was used to replace the computed-torque scheme for robot control in the joint space.

The input commands in all the experiments were step commands. The actuator force of each actuator is constrained by its physical limits, so that saturation will occur if the controller output is large. To remedy the saturation problem, the speed-constraint function (Khatib, 1987) was joined to the controller for the large step command. This function is described as follows:

$$a^* = K_{Dr}\left[-\dot{r} + K_{Pr}K_{Dr}^{-1}V(r_d - r)\right] \quad (37)$$

where

$$V = \min(1, \frac{V_{max}}{\frac{k_{pr}}{k_{dr}} \parallel r_d - r \parallel}). \quad (38)$$

k_{pr} and k_{dr} are the diagonal elements of K_{Pr} and K_{Dr}, respectively. V_{max} is the maximum velocity. Here, $V_{max} = 0.1$ m/s. The controller parameters were defined as follows: $K_P = 64I$, $K_D = 16I$, the sampling period was 3 ms. ρ of the DARAC and ρ_r of the DRRAC were both chosen to be the same as eq. (28).

Experiment 1 illustrates the responses of the manipulator when there was an unreachable region between the desired position and the initial position. The orientation was ignored. The initial and target positions were (−0.1, 0.2, 0.8) and (0.15, −0.15, 0.8), respectively; they are illustrated in Fig. 6. The singular circle in the figure is the boundary of the workspace, the unreachable region is inside it, and the workspace of the manipulator is outside it. The positional errors of the DARAC and the DRRAC are shown in Figs 7(a) and (b), respectively. From these two figures, it was found that the positional errors of the two methods had converged to zero, though the convergent rate of the DARAC was faster than that of the DRRAC. After the end-effector had touched the circle, there were some fluctuations around the singular circle when the DARAC was used. For the DRRAC, the trajectory just had one very slight fluctuation, since the unnecessary joint velocities were removed. However, the convergent rate of the DRRAC was slow when the target was close to the singular point. This occurred because the joint velocities along the degenerated directions were damped when the end-effector moved into the neighborhood of the singularity.

In Experiment 2, the target was outside the workspace of the manipulator. The initial position was (−0.1, 0.2, 0.8) and the target was (−0.05, 0.05, 0.8); these are illustrated in Fig. 8. The positional errors of the DARAC and the DRRAC are shown in Fig. 9. When the DARAC was used, after the end-effector had touched the singular circle, fluctuations occurred around the workspace boundary. However, when the DRRAC was used, after the end-effector had touched the circle, the end-effector moved along the workspace boundary without fluctuations. Finally, the end-effector converged to the singular point nearest to the target.

Experiment 3 illustrates the response of the manipulator in the face of orientation degeneration. The initial position and the target were (−0.1, 0.2, 0.8) and (−0.0203, 0.1501, 0.8649), respectively. The orientation was held towards the +Z axis. At the target, q_5 was zero, i.e., a singular point. The joint displacements of the joints 4, 5, and 6 for the DARAC are shown in Fig. 10(a). In this figure, when $q_5 = 0$, joints 4 and 6 rotated at the same speed in the opposite directions. This is because the DARAC forces $\ddot{q}_4^*$ and $\ddot{q}_6^*$ to zero when $q_5 = 0$; however, $\dot{q}_4$ and $\dot{q}_6$ were nonzero. The results with the DRRAC are shown in Fig. 10(b). When q_5 approached 0, both joints then stopped at the same time.

The results of these three experiments show that the proposed method also has satisfactory results even if the perfect computed-torque scheme is not used.

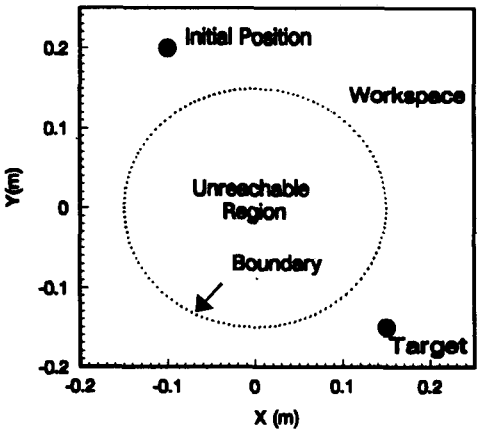

Fig. 6. The initial position and the target position for Experiment 1.

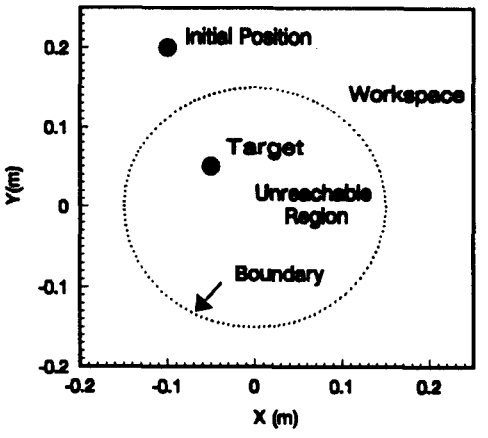

Fig. 8. The initial position and the target position for Experiment 2.

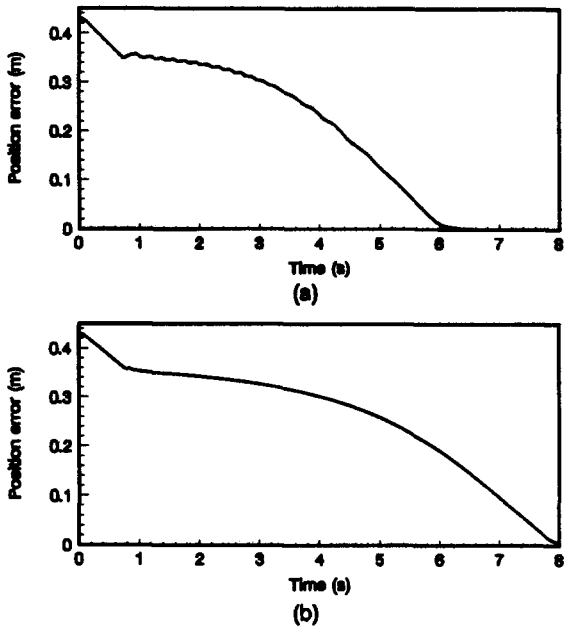

Fig. 7. Experiment 1; the positional errors of (a) DARAC and (b) DRRAC.

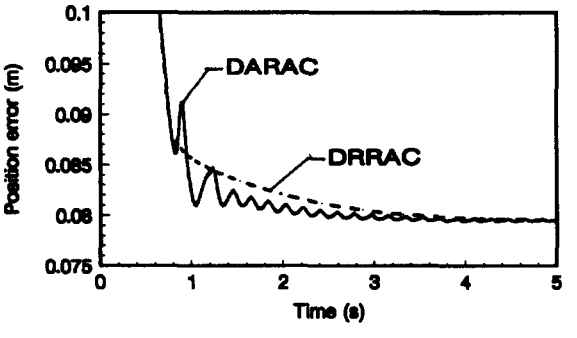

Fig. 9. Experiment 2; the positional errors of DARAC and DRRAC.

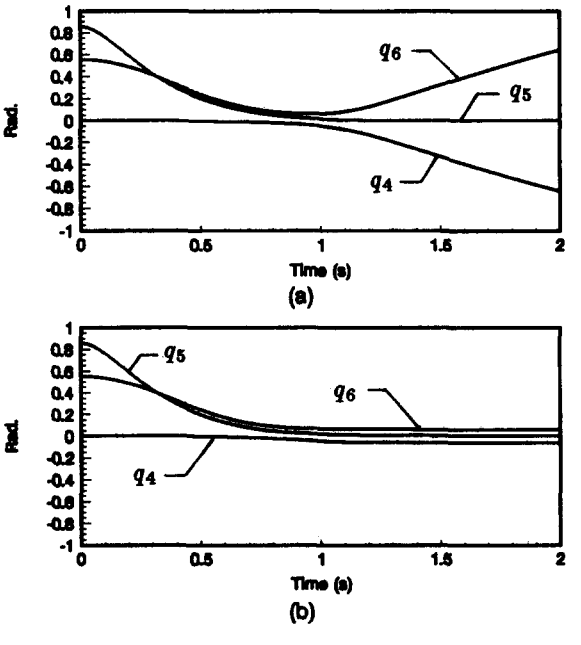

Fig. 10. Experiment 3; the histories of q_4, q_5, q_6 of (a) DARAC, (b) DRRAC.

6. CONCLUSION

This paper has presented the DRRAC to overcome the motion problems of the DARAC in the neighborhood of a singular point. The proposed method directly damps the velocities instead of the accelerations, such that unnecessary joint velocities are removed at the singular point. The DRRAC solves the fluctuation and self-motion problems of the DARAC. That the proposed control scheme is asymptotically stable is also proved in this paper. Three experimental results show that the DRRAC makes the resolved-acceleration control scheme more practical for using in indus-

trial manipulators.

The main advantage of the DRRAC is that the robot control system does not need to plan its path to avoid the unreachable region, since the controller will command the end-effector to move along the boundary of the workspace with the minimum trajectory error if the desired path is outside the workspace. Also, the proposed approach is so simple that it can easily upgrade the existing acceleration control technique by improving the performance of the motion in the neighborhood of the singularity. An insignificant drawback of the DRRAC is that if the target is in the neighborhood of a singularity, then a small error will remain for a long decaying period. This problem will be resolved in future work.

ACKNOWLEDGMENTS

The authors are grateful for the support of the National Science Council, Taiwan, under Grant NSC83-0422-E-009-066.

REFERENCES

Chiaverini, S. (1993). Estimate of the two smallest singular value of the Jacobian matrix: application to damped least-squares inverse kinematics. *J. Robotic Systems,* vol. 10, no. 8, pp. 991-1008.

Chiaverini, S., B. Siciliano, and O. Egeland (1994). Review of the damped least-squares inverse kinematics with experiments on an industrial robot manipulator. *IEEE Tran. Control Systems Technology,* vol. 2, no. 2, pp. 123-134.

Deo, A. S., and I. D. Walker (1995). Overview of damped least-squares method for inverse kinematics of robot manipulators. *J. Intelligent and Robotic Systems,* vol. 14, pp. 43-68.

Hsia, T. C., T. A. Lasky, and Z. Guo (1991) Robust independent joint controller design for industrial robot manipulators. *IEEE Trans. Industrial Electronics,* vol. 38, no. 1, pp. 21-25.

Khatib, O. (1987). A unified approach for motion and force control of robot manipulators: the operational space formulation. *IEEE J. Robotics and Automation,* vol. 1, pp. 45-53.

Kirćanski, M. and M. Borić (1993). Symbolic singular value decomposition for a PUMA robot and its application to a robot operation near singularities. *Int. J. Robotics Research,* vol. 12, no. 5, pp. 460-472.

Kirćanski, M., N. Kirćanski, Dj. Leković, and M. Vukobratović (1994). An experimental study of resolved acceleration control in singularities: damped least-squares approach. *Proc. IEEE Int. Conf. Robotics and Automation,* pp. 2686-2691.

Lin, S. K. (1995). Robot control in Cartesian space. In: *Progress in Robotics and Intelligent Systems,* (G. W. Zobrist and C. Y. Ho Ed.), vol. 3, pp. 85-124. New Jersey: Ablex.

Lin, S. K. and S. L. Wu (1995). Implementation of the damped resolved acceleration control for a manipulator near singularity. *J. Systems Engineering,* vol. 5, no. 3, pp. 174-191.

Luh, J. Y. S., M. W. Walker, and R. P. Paul (1980). Resolved-acceleration control of mechanical manipulators. *IEEE Trans. Automatic control,* vol. AC-25, pp. 195-200.

Maciejewski, A. A. and Ch. A. Klein (1988). Numerical filtering for the operation of robotic manipulators through kinematically singular configurations. *J. Robotic Systems,* vol. 5, no. 6, pp. 527-552.

Maciejewski, A. A. and Ch. A. Klein (1989). The singular value decomposition: computation and applications to robotics. *Int. J. Robotics Research,* vol. 8, no. 6, pp. 63-79.

Nakamura, Y. and H. Hanafusa (1986). Inverse kinematic solutions with singularity robustness for robot manipulator control. *Trans. ASME J. Dynamic Sys., Meas., Contr.,* vol. 108, pp. 163-171.

Spring, K. W. (1986). Euler parameters and the use of quaternion algebra in the manipulator of finite rotations: A review. *Mechanism and Machine Theory,* vol. 21, no. 5, pp. 365-373.

Tsai R., S. K. Lin (1990). Design and implementation of the torque control for a DC servo. *Proc. 14th National Symp. Automatic Control,* Taiwan, pp. 565-572.

Wampler, C. W. (1986). Manipulator inverse kinematic solution based on vector formulations and damped least-squares methods. *IEEE Trans. Sys., Man, Cybern,* vol. 16, no. 1, pp. 93-101.

Wampler, C. W. and L. J. Leifer (1988). Applications of damped least-squares methods to resolved-rate and resolved-acceleration control of manipulators. *ASME J. Dynamic Sys., Meas., Contr.,* vol. 110, pp. 31-38.

Wu, S. L. and S. K. Lin (1994). A modular integrated robot control system. *Proc. 4th IFAC Symposium on Robot Control,* vol. 1, pp. 283-288.